Fine thermal structure of a coronal active region from Hinode/XRT

Fabio Reale[1,2], Susanna Parenti[3], Kathy K. Reeves[4], Mark Weber[4], Monica G. Bobra[4], Marco Barbera[1,2], Ryohei Kano[5], Noriyuki Narukage[6], Masumi Shimojo[7], Taro Sakao[6], Giovanni Peres[1,2], Leon Golub[4]

ABSTRACT

Hinode/XRT observations in several different filters allow us for the first time to resolve the fine thermal structure of a coronal active region on the Sun.

The determination of the fine thermal structure of the solar corona is fundamental to constrain the coronal heating mechanisms. Hinode/XRT collects images of the solar corona in different passbands, thus providing temperature diagnostics through hardness ratios. We have devised a hardness ratio combining different filters which optimizes the signal-to-noise ratio. The application of this technique to a coronal active region observed in five filters reveals a highly thermally-structured corona: very fine structures in the core of the region and on a larger scale further away. We notice continuous thermal distribution along the coronal loops, but also evidence of interacting structures, and variations of thermal structuring along the line of sight. The latter ones are confirmed by the comparison with the region as imaged with TRACE, sensitive to cooler plasma emission.

---

[1]Dipartimento di Scienze Fisiche ed Astronomiche, Sezione di Astronomia, Università di Palermo, Piazza del Parlamento 1, 90134 Palermo, Italy

[2]INAF/Osservatorio Astronomico di Palermo, Piazza del Parlamento 1, 90134 Palermo, Italy

[3]Royal Observatory of Belgium, 3 Circular Avenue, B-1180 Brussels, Belgium

[4]Harvard-Smithsonian Center for Astrophysics, Cambridge, MA 02138, USA

[5]National Astronomical Observatory, Mitaka, Tokyo 181-8588, Japan

[6]Institute of Space and Astronautical Science, Japan Aerospace Exploration Agency, 3-1-1 Yoshinodai, Sagamihara, Kanagawa 229-8510, Japan

[7]Nobeyama Solar Radio Observatory, National Astronomical Observatory, Nobeyama, Nagano 384-1305, Japan

Measuring the temperature in the solar corona.

The solar corona is highly structured by the solar magnetic field and it is widely accepted that the origin of the heating of the million degree plasma confined in the closed coronal structures (named *loops*) lies in the magnetic field (e.g Vaiana et al. 1973). However, the high efficiency of the thermal conduction in the coronal plasma prevents a direct diagnosis of the detailed mechanisms which convert the magnetic energy into thermal energy. The determination of the fine thermal structure of the corona is a crucial issue to solve the question of the detailed origin of the coronal heating. For instance, it is currently under debate whether frequent small and rapid heating episodes (the so-called nanoflares, e.g. Parker 1988, Cargill 1994, Cargill & Klimchuk 2004) are entirely able to heat the solar corona or partly or only negligibly (Klimchuk 2006). The solar active regions are good laboratories to investigate these kinds of things, because they include a wide variety of structures and can be the object of systematic studies. On the other hand, they are the most complex X-ray emitting regions of the Sun, in which the structures at all scales interact and overlap with each other. This makes it very difficult to disentangle the details of each coronal structure from the others.

So far, one problem that has seriously limited our insight into the coronal heating problem has been the relatively poor resolution of the diagnostics of the thermal structure in coronal regions. We haven't been able to assess the filamentation of the thermal structuring, nor the distribution of the thermal components along the line of sight, i.e. across the coronal loops. Only through information on the detailed thermal structure can we assess the details of the heating distribution in the coronal loops. Some hints for the fine thermal configuration of coronal regions were obtained from investigation of the emission measure distribution derived from spectral observations (e.g. Dere & Mason 1993, Landi & Landini 1998) and from multi-band imaging of a high-resolution UV telescope, i.e. TRACE (e.g. Reale & Ciaravella 2006), but no direct evidence has been obtained so far. On the other hand, a fine thermal structuring would be fundamental to put a conclusive word on the fine details of the coronal heating.

The aim of this study is to investigate the detailed thermal structure of a solar coronal active region, by exploiting the diagnostics coming from the observations in several wide-band X-ray filters from the Hinode/X-Ray Telescope (XRT, Golub et al. (2007)).

The Hinode/XRT observation of the active region.

The instrument XRT on board Hinode is a grazing-incidence soft X-ray telescope, which is sensible to the emission of plasma in the temperature range $6.1 < log\ T < 7.5$. Several temperature passbands are provided by a selection over nine different filters in the X-ray band plus one in the G band continuum . These are held in two filter weels (FW1 and FW2) located close to the focal plane in front of the CCD camera. The latter has a 1 arcsec pixel and the resulting PSF is 0.8 arcsec wide. More details on the instruments are found in Golub et al. (2007).

We observed AR 07993 while it was located close to the Sun center, using Hinode/XRT telescope with a field of view of 512×512 arcsec^2. The data were obtained on the 12 November 2006, by using sequences of five positions for FW1 combined with the FW2 in the 'Open' position. The filters used were: Al_poly (exposure time 0.26 s), C_poly (0.36 s), Be_thin (1.44 s), Be_med (8.19 s) and Al_med (16.38 s). The observation dataset used for this analysis covers one hour, starting at 13:00, with a cadence for each filter of five minutes. This active region was monitored by XRT all along its passage from the east to the west limb. It flared several time during this period. However, during the selected hour no major flare and no significant rearrangement of the region morphology occurred. We used the standard XRT software (XRT_PREP, 'v2007.May.19') to perform the Level-1 calibration. This includes corrections for the read-out signal, flat-field, CCD bias. The observation images are finally co-aligned with a cross-correlation technique.

Fig. 1 shows the region as imaged with the XRT. This image results from a geometric mean of five frames, one for each filter. Each frame is the average of 12 frames taken at equispaced interval during the selected hour of observation. This image therefore maximizes the signal-to-noise ratio, at the cost of cancelling out the temporal variations of each structure and therefore with the risk of diffusing the structures. The figure cuts off the signal fainter than 10 DN pixel^{-1} s^{-1}. We can distinguish several interesting features: a main toroidal loop arcade ($\sim$ 100 arcsec wide, labelled A, B and C in Fig. 1) surrounding the central black magnetic pole, open to the south, large scale loops (up to more than 350,000 km long, L in Fig. 1) in the south-west and north regions, a bright knot south of the magnetic pole ($(X,Y) \approx [270,220]$ arcsec, K in Fig. 1), an upside-down V-like loop system on the right of the bright knot ($(X,Y) \approx [300,240]$ arcsec, V in Fig. 1). The brightest part of the region is the loop system right in the center of the picture ($(X,Y) \approx [220,230]$ arcsec, X in Fig. 1). The figure already clearly shows a high degree of loop substructuring and most loops intersect along the line of sight.

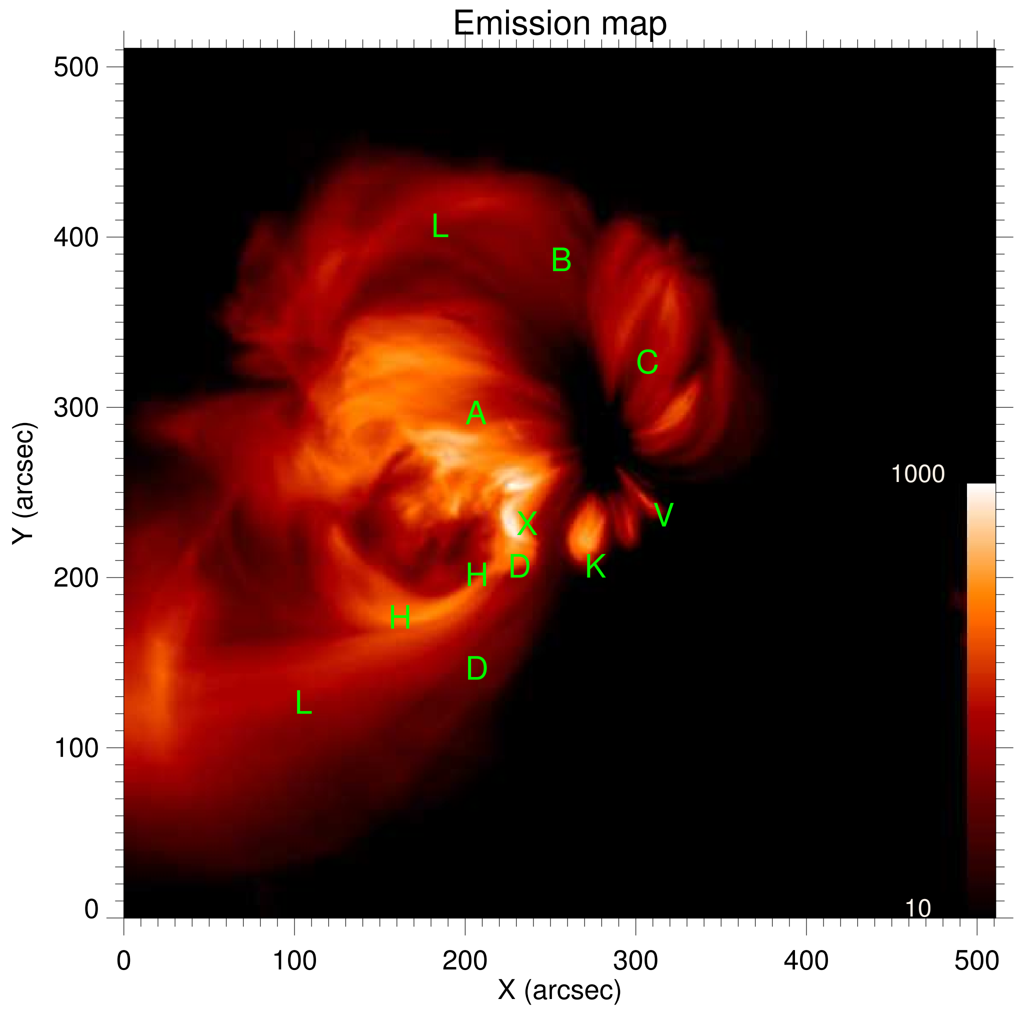

Fig. 1.— Emission image of the active region AR 07993 as observed with the Hinode/XRT. The image is the result of a geometric mean of all frames taken in the five filters during an hour. The red color scale is logarithmic in the range indicated in the palette.

Filter ratios to measure the coronal temperature

In order to extract thermal information from the XRT images we exploit the property of the emission of the optically thin plasma of being a separated function of the temperature and the density. The emission of an isothermal element of plasma is proportional to the square of its density times the element volume (the so-called emission measure), times a relatively weak function of the temperature (plasma emissivity). Each filter has a different passband and therefore a different response to plasma temperature, so that we can define a filter temperature response function which replaces the plasma emissivity.

The emission of an optically thin isothermal plasma as measured in a j-th XRT filter passband is:

$$I_j = EM \quad G_j(T) \tag{1}$$

where T is the temperature and EM is the emission measure, defined as

$$EM = \int_V n^2 dV$$

where n is the particle density, and V the plasma volume. Fig. 2 shows the temperature response of the five XRT filters used in this observation, in arbitrary units.

The ratio of the emission in two different filters is then independent of the density, and only a function of the temperature:

$$R_{ij} = \frac{I_i}{I_j} = \frac{G_i(T)}{G_j(T)} \tag{2}$$

The inversion of this relationship provides a value of temperature (Vaiana et al. 1973). For selected pair of filters it is then possible to have a unique correspondence between the filter ratio value and the temperature.

In the light of this property, if two images of the same region are taken in two different filters, the ratio of the images provides a temperature map. For non-isothermal plasma along the line of sight, the ratio no longer provides an exact temperature value but still it remains an average temperature indicator, weighted for the emission measure. The standard approach is to select various couples of filters and derive related temperature maps. The temperature map obtained from the ratio of two filter images is typically affected by the summation of the statistical fluctuations of each emission image and, as a result, it is much more diffuse, so that the structures on fine spatial scales are smoothed out (e.g Tsuneta et al. 1992, Yoshida & Tsuneta 1996). This effect has prevented so far the investigation of

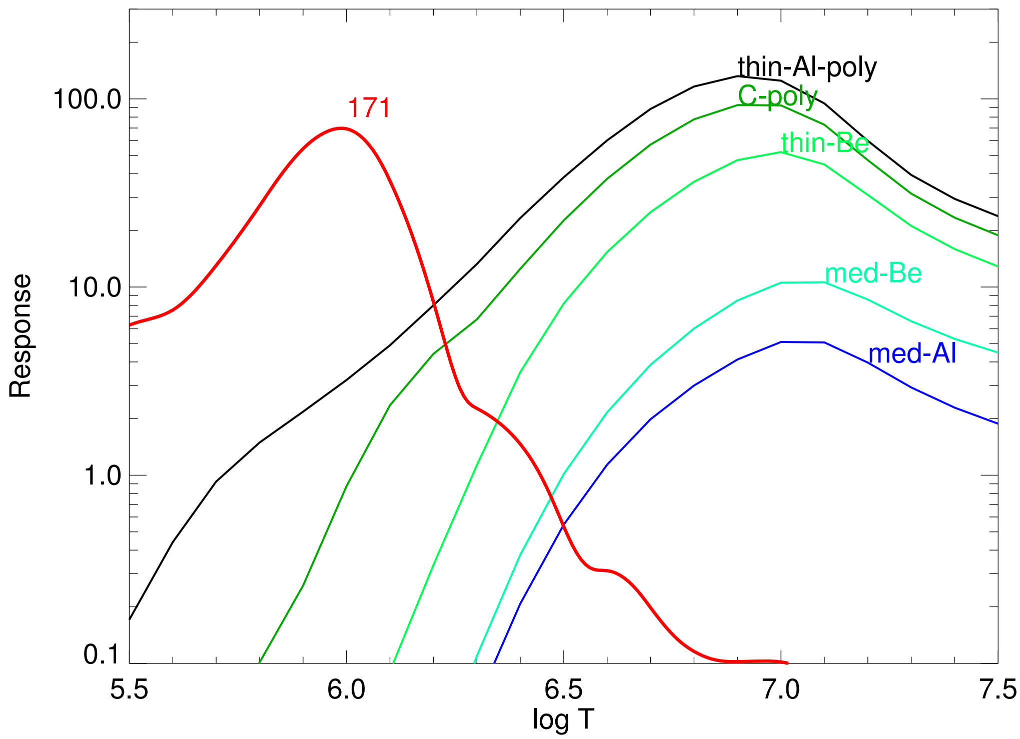

Fig. 2.— Temperature response function of the five XRT filters used in this observation and of the TRACE 171 A filter, in arbitrary units.

the thermal structuring of the confined corona down to spatial scales of the order of the instruments resolution.

With respect to the previous existing instruments, XRT both improves the nominal resolution in the soft X-ray band down to about one arcsec and makes available several broadband filters with different temperature sensitivity. In order to fully exploit these achievements we have devised a filter ratio obtained from a combination of the available filters, which significantly improves the signal-to-noise ratio and the spatial resolution of the thermal maps. The basic point is to consider the geometric mean of the emission in all the filters available and divide by the emission in one filter. The geometric mean allows us to normalize for the different level of sensitivity of the soft and hard filters, enhancing the statistics of the regions where the signal is high in most filters. A further enhancement of the signal-to-noise ratio is obtained by considering the product of the ratios computed for the two softest filters, i.e. Al_poly and C_poly, thus improving also the denominator of the filter ratio.

Result: the thermal map

Fig. 3 shows the thermal map of the region of Fig. 1 obtained with the just described combination of filter ratios. In the green linear color scale, indicatively, bright is hot and dark is cool. We have excluded all pixels with low signal ($\leq$ 100 DN/s) in the two softest filters, i.e. Al_poly and C_poly. The first striking result immediately apparent in this figure is the very high degree of thermal structuring in the core loop arcade, even more evident than in the emission map. The thickness of the structures clearly goes down to the order of the instrument resolution ($\sim$ 2 pixels). On the right side of the arcade (region C in Fig. 1) we observe that the loops are disposed in an ordered sequence with small overlap between each other. A continuous thermal distribution can be clearly traced along each of these loops. On the left side (region A), we see a much higher level of overlap and even tangling of the thin loop components. This is the region which flared several times during the entire campaign of XRT observation. The bright knot (K) well isolated in the emission image is here clearly linked to the left side of the arcade and is bounded by a very thin bright ring. The V-like loop system (V) is very bright, indicating hot confined plasma. Although still clearly structured, the thermal distribution appears less organized in the region on the left of arcade A. In general, the loops entirely visible exhibit a hot (bright) apex and a cooling trend along both legs, as expected from standard loop models (e.g. Vesecky et al. 1979, Serio et al. 1981).

In region L on the bottom-left of the figure, we see that the largest scale structures are also mostly on the brighest side of the color scale. Some substructuring is also resolved but

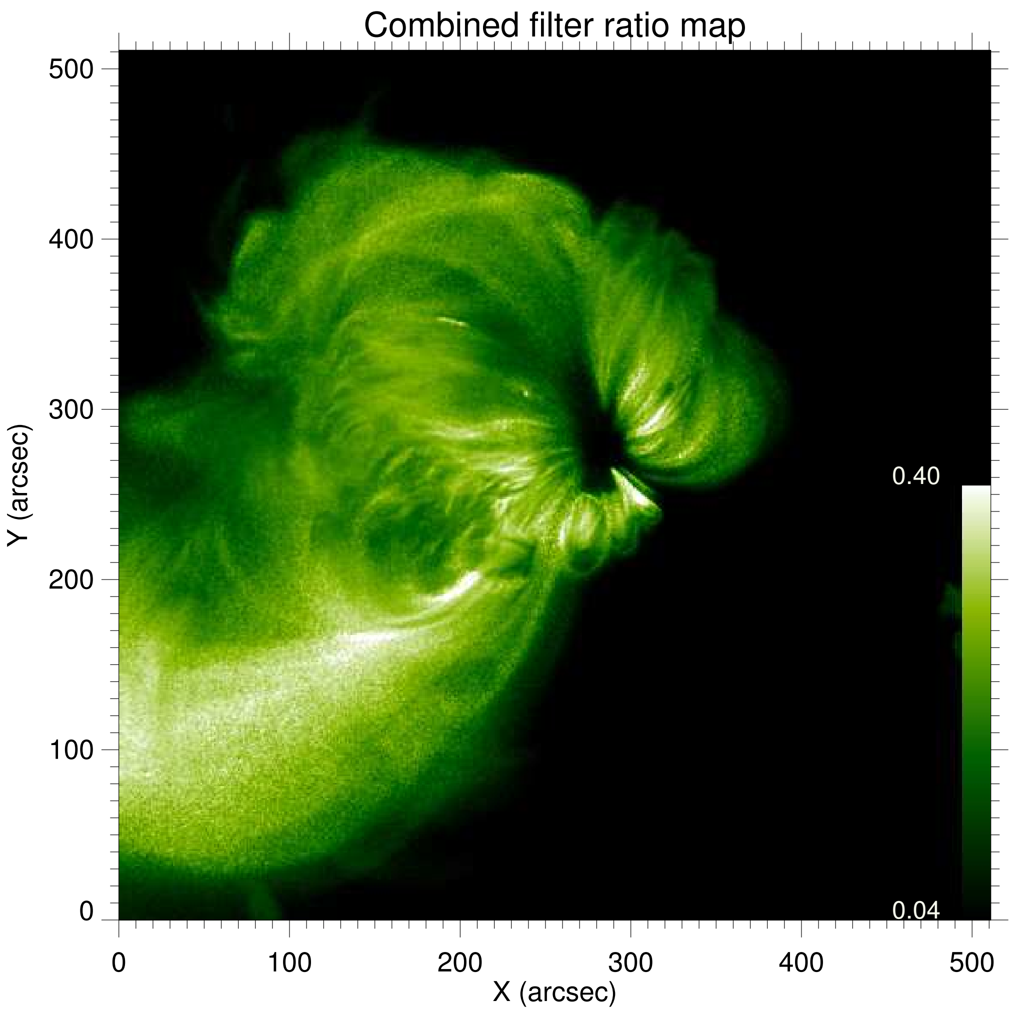

Fig. 3.— Thermal map of the active region in Fig. 1 derived from a combined filter ratio as described in the text. The green scale is linear in the range indicated in the palette and with the temperature correspondence plotted in Fig. 4.

on larger scale size; the granularity in this region is related to the lower count statistics and does not allow us at the moment to decide whether the lower level of substructuring is real or due to low sensitivity.

Fig. 4 shows the temperature calibration scale of the thermal map. According to this plot, the dependence of the combined filter ratio is almost linear on $\log T$. In view of Fig. 4, assuming an isothermal plasma along the line of sight (*solid line*), the temperature range of this active region plasma would be $6.15 \leq \log T \leq 6.6$. However, we cannot ignore the possibility that the plasma is non-isothermal along the line of sight. Fig. 4 exhibit possible variations of the combined filter ratio values due to this effect. In particular, an excess of hot plasma along the line of sight leads to a significant increase (~ 0.02 for the selected example, *dashed line*) of the ratio value, an excess of cool plasma to a decrease ($\sim 0.005 - 0.01$, *dot-dashed line*) of it.

If we go back to examine Fig.3, we realize that in some regions the effects are clearly present, while in others, for contrast, much less. Bright excesses are associated with the overlap of different large loops (e.g. regions H in Fig. 1, $(X, Y) \sim [200, 200]$ arcsec, $(X, Y) \sim [150, 170]$ arcsec) and the thin strands in the core region (A). This can be immediately recognized in the thermal map from the steep unexpected change of color (brightening) along the loops, with no significant correspondence in the emission map (Fig.1). Relative darkenings (e.g. regions D in Fig. 1, $(X, Y) \sim [230, 200]$ arcsec, $(X, Y) \sim [200, 140]$ arcsec) clearly break otherwise smooth ratio distributions along the large loop systems. Such darkenings are also present in the knot (K), in the right side of the loop arcade (C, $(X, Y) \sim [320, 300]$ arcsec), and a very large one at the base of the north part of the arcade (region B). Therefore, we are able to distinguish directly regions where the emission measure distribution along the line of sight is broader and also whether the plasma excess is cool or hot.

Fig. 5 shows that this scenario is reliable: on the data from Fig. 3 we superimpose the brightest features imaged simultaneously by the TRACE (171 A filter) telescope, which is sensitive mostly to cooler plasma around 1 MK (Fig. 2). The map shows that the darkened spots (D and B) have a clear correspondence to bright regions in the TRACE image, i.e. there is an excess of cool plasma along the line of sight.

Conclusions

The map shown in Fig. 3 represents a significant achievement from the Hinode/XRT experiment: it shows directly the existence of thermally coherent thin magnetic structures

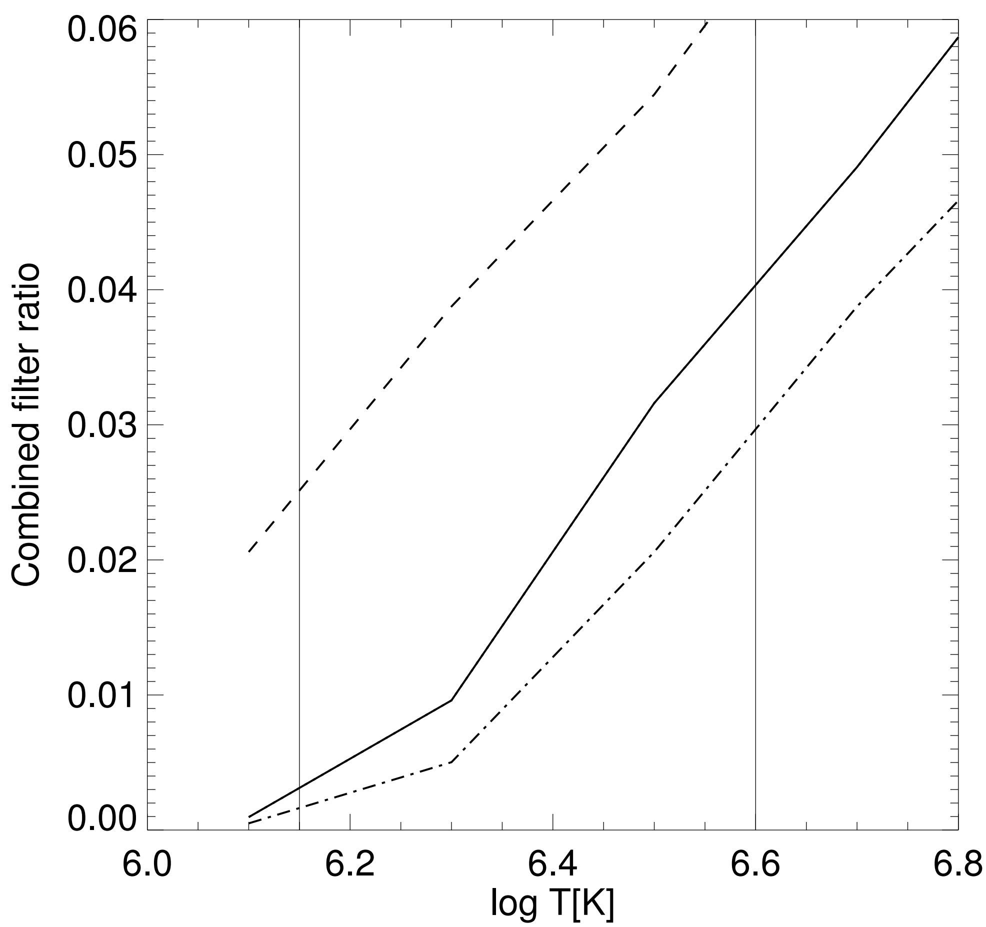

Fig. 4.— Combined filter ratio vs temperature, as predicted for isothermal plasma (*thick solid line*) and for broader emission measure distributions along the line of sight, i.e. with hot excess (flat emission measure extended to $\Delta \log T = +0.45$, *dashed line*) and cool excess (flat emission measure extended to $\Delta \log T = -0.45$, *dot-dashed line*). The approximate range of the color scale of Fig. 3 is marked (*vertical lines*).

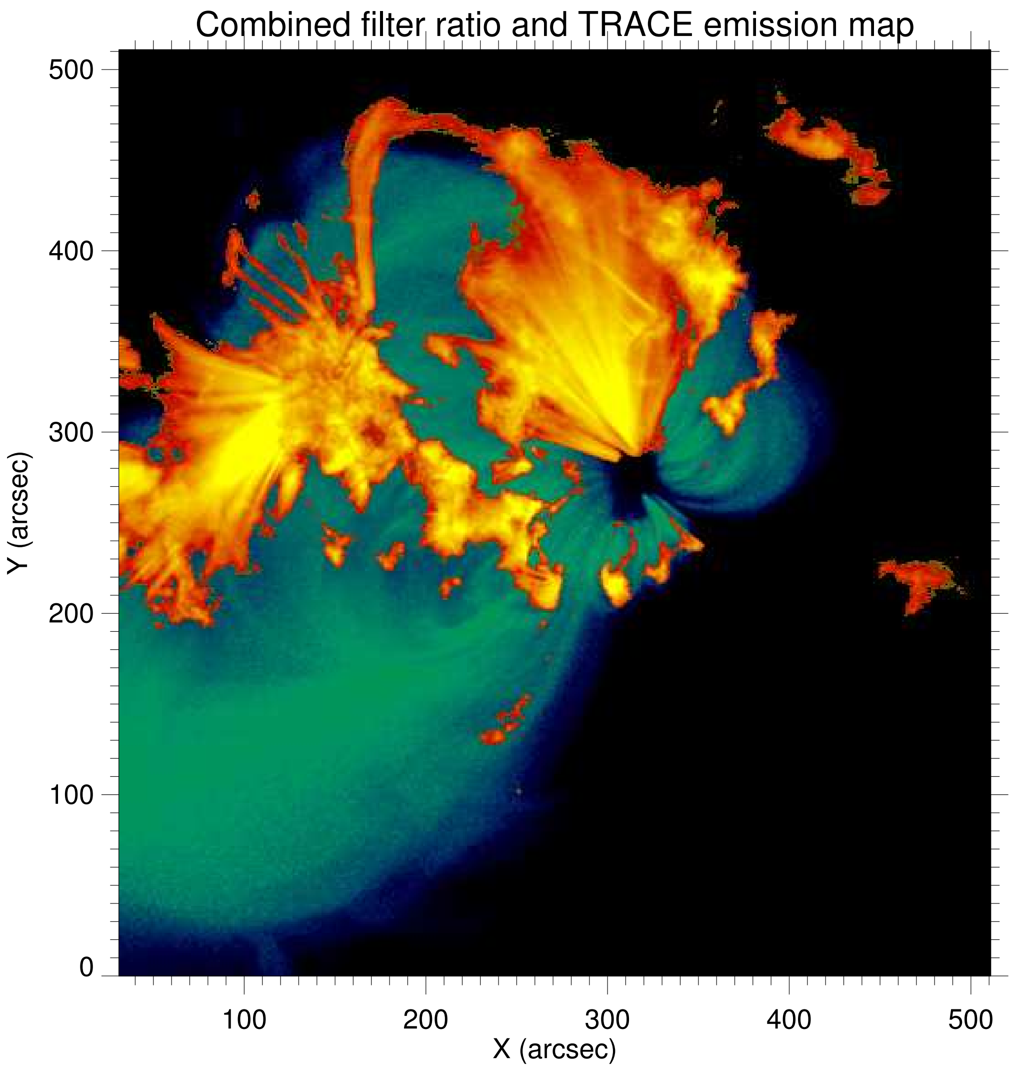

Fig. 5.— Same as Fig. 3 superimposed with a emission map taken simultaneously with the TRACE telescope in the 171 A filter passband (sensitive to ~ 1 MK plasma). The TRACE emission above 1.5 DN pixel^{-1} s^{-1} is shown.

and that hot coronal loops are highly transversally structured. The tightness of the thin structures in the left side of the core loop arcade suggests that these structures probably interact with each other and, therefore, that we are seeing a direct signature of the heating mechanisms themselves (Lopez Fuentes et al. 2006, Klimchuk 2006). This result could be obtained taking full advantage both of the unprecedented spatial resolution in the X-rays and of the several filters available. The relative similarity of the filter temperature sensitivity makes the procedure of averaging and combination into the above described filter ratio particularly fruitful in enhancing the signal-to-noise ratio.

Thanks to the high resolution achieved we could also address new diagnostics: the direct evidence of multi-thermal structuring along the line of sight with the impressive correspondence to structures imaged by the telescope TRACE, sensitive to cooler plasma.

The present study opens a whole new line of investigation. In particular, it will be possible to study the details of the thermal structuring, and its time variations and to conduct systematic studies of the thermal distribution both along the line of sight and along the structures in entire regions.

Hinode is a Japanese mission developed and launched by ISAS/JAXA, with NAOJ as domestic partner and NASA and STFC (UK) as international partners. It is operated by these agencies in co-operation with ESA and NSC (Norway). FR, GP and MB acknowledge support from Italian Ministero dell'Università e Ricerca and Agenzia Spaziale Italiana (ASI). US members of the XRT team are supported by NASA contract NNM07AA02C to SAO. SP acknowledge the support from the Belgian Federal Science Policy Office through the ESA-PRODEX programme. This work was partially supported by the International Space Science Institute in the framework of an international working team.

REFERENCES

Cargill, P. J. 1994, ApJ, 422, 381

Cargill, P. J., & Klimchuk, J. A. 2004, ApJ, 605, 911

Dere, K. P., & Mason, H. E. 1993, Sol. Phys., 144, 217

Golub, L. et al., 2007, Sol. Phys., in press

Klimchuk, J. A. 2006, Sol. Phys., 234, 41

Landi, E., & Landini, M. 1998, A&A, 340, 265

López Fuentes, M. C., Klimchuk, J. A., & Démoulin, P. 2006, ApJ, 639, 459

Parker, E. N. 1988, ApJ, 330, 474

Reale, F., & Ciaravella, A. 2006, A&A, 449, 1177

Serio, S., Peres, G., Vaiana, G. S., Golub, L., & Rosner, R. 1981, ApJ, 243, 288

Tsuneta, S., Hara, H., Shimizu, T., Acton, L. W., Strong, K. T., Hudson, H. S., & Ogawara, Y. 1992, PASJ, 44, L63

Vaiana, G. S., Krieger, A. S., & Timothy, A. F. 1973, Sol. Phys., 32, 81

Vesecky, J. F., Antiochos, S. K., & Underwood, J. H. 1979, ApJ, 233, 987

Yoshida, T., & Tsuneta, S. 1996, ApJ, 459, 342